Strategic and operational decision-making in expanding supply chains for LNG as a fuel

Lopez Alvarez, Jose A.; Buijs, Paul; Deluster, Rogier; Coelho, Leandro C.; Ursavas, Evrim

Published in:
Omega: International Journal of Management Science

DOI:
10.1016/j.omega.2019.07.009

Strategic and operational decision-making in expanding supply chains for LNG as a fuel

Jose A. Lopez Alvarez[a], Paul Buijs[a,*], Rogier Deluster[a], Leandro C. Coelho[a,b], Evrim Ursavas[a]

[a] *University of Groningen, Faculty of Economics and Business, Department of Operations, The Netherlands*
[b] *Canada Research Chair in Integrated Logistics, Université Laval, Canada*

Abstract

The European Union aims for a 40% reduction in greenhouse gas emissions by 2030, compared to 1990 levels, and recognizes the opportunities of Liquefied Natural Gas (LNG) as an alternative fuel for transportation to reach this goal. The lack of a mature supply chain for LNG as a fuel results in a need to invest in new (satellite) terminals, bunker barges and tanker trucks. This network design problem can be defined as a Two-Echelon Capacitated Location Routing Problem with Split Deliveries (2E-CLRPSP). An important feature of this problem is that direct deliveries are allowed from terminals, which makes the problem much harder to solve than the existing location routing literature suggests. In this paper, we improve the performance of a hybrid exact algorithm and apply our algorithm to a real-world network design problem related to the expansion of the European supply chain for LNG as a fuel. We show that satellite terminals and bunker barges become an interesting option when demand for LNG grows and occurs further away from the import terminal. In those situations, the large investments associated with LNG satellites and bunker barges are offset by reductions in operational costs of the LNG tanker trucks.

Keywords: sustainability, alternative fuel, liquefied natural gas (LNG), network design problem, neighborhood search, exact algorithm

1. Introduction

Through its Alternative Fuels Directive 2014/94/EU, the European Commission is seeking to promote the deployment of alternative fuel infrastructures to enable an increase in the uptake of alternative fuel vehicles. Among the currently available alternative fuels, Liquefied Natural Gas (LNG) is widely considered to be the best option for long-haul road-freight and maritime transportation. LNG is natural gas that is converted to a liquid state by cooling it down to approximately $-162\,^{\circ}\mathrm{C}$. In this liquid state, it takes up much less volume compared to a (compressed) gaseous state, which makes LNG particularly suitable as a fuel for long-haul transportation. Using LNG as a transportation fuel is a recent development, and the supply

*Corresponding author

Email addresses: j.a.lopez.alvarez@rug.nl (Jose A. Lopez Alvarez), p.buijs@rug.nl (Paul Buijs), r.deluster@student.rug.nl (Rogier Deluster), leandro.coelho@cirrelt.ca (Leandro C. Coelho), e.ursavas@rug.nl (Evrim Ursavas)

chain through which the fuel is made available to its customers is still noticeably in development [35, 26].

In the last few years, the European LNG supply chain has been quickly expanding. Many LNG fuel stations have been opened and several ports can now supply ships with LNG as a fuel. The LNG is supplied from large import terminals, where specialized tanker trucks and bunker barges can load the LNG that is to be transported to fuel stations and ports. Since there are only a few, very large import terminals around the world, new (smaller) satellite terminals may need to be opened to efficiently transport LNG to ports and fuel stations in areas located further from the import terminals. Deciding whether to open one or more terminals, and if so, to determine their locations and sizes, are critically important decisions in the development of LNG supply chains, and may have a profound impact on the routing decisions of the tanker trucks and bunker barges. For the longer-term viability of the market for LNG as a fuel, it is critically important to make only the necessary investments, as any excess investment will have a negative impact on the price custumers pay for the fuel.

This paper presents a new problem aimed at finding an efficient and cost-effective network design for fulfilling the demand for LNG as a fuel. The network can consist of two types of facilities: import terminals, which serve as the initial source of LNG for the whole network, and smaller-sized satellite terminals, which serve as intermediate facilities. Opening a facility is associated with an investment cost, and if opened, there are operating costs per unit volume of LNG. The facilities have a given capacity that can be upgraded at an additional investment cost. By Using tanker trucks and bunker barges as modes of transportation, the LNG can be transported from an import terminal to the demand points directly, or via a satellite terminal. Each of these vehicle types has a given capacity and is associated with a certain fixed and variable cost. The problem is to open and/or upgrade facilities, to decide upon the routes of the tanker trucks and bunker barges, and to allocate inventories, while minimizing facility and transportation costs over multiple periods.

The problem we study consists of attributes that have not been considered in combination in previous studies. The concept of simultaneously determining location and routing decisions was put forward by Boventer [7], Maranzana [20] and Watson-Gandy and Dohrn [37] which led to the research field known as the location-routing problem (LRP). Surveys on this topic are published by Min et al. [22], Nagy and Salhi [24], Balakrishnan et al. [4], Prodhon and Prins [30] and Drexl and Schneider [10]. In the past decades, numerous extensions to the LRP have been identified. Karaoglan et al. [15], for example, worked on the LRP with simultaneous pickup and delivery by means of a branch-and-cut algorithm. Prins et al. [27] considered capacitated routes and depots in an LRP structure. Several papers address a multi-period setting. Prodhon [29] uses visiting patterns to customers and assigns customers to facilities for each period. A customer can be visited from different depots over time. Albareda-Sambola et al. [3] worked on the dynamic LRP and by considering different scales within the time horizon reflected on the stability of location decisions as compared to routing decisions. Schiffer and Walther [33] study a network design problem for electric logistics fleet in which location and routing decisions are considered. The authors studied a setting where customers induce uncertainty in terms of geographical distribution, time windows and demand.

To solve the variety of LRPs different techniques based on heuristic methods and exact algorithms have been developed [2, 12, 14, 16, 18, 21]. Contardo et al. [8] developed an exact technique based on cut and column generation. They introduced a new set of inequalities and tested instances from Perl and Daskin [25], Tuzun and Burke [36], Barreto [6], Prins et al. [28], Akca et al. [1] and Baldacci et al. [5] and improved the bounds found in the literature. In a recent work, Schneider and Löffler [34] developed a tree-based search heuristic that uses a large composite neighborhood.

An important attribute when studying the LRPs is the hierarchical structure of the network and the existence of intermediate facilities [32]. Considering this, Guastaroba et al. [13] provided a survey on transportation problems where the presence of intermediate facilities a has significant influence on cost and distribution structure. A survey of two-echelon LRPs has been published by Cuda et al. [9]. Rieck et al. [31] studied a LRP where pickup and deliveries are performed on local multi-stop routes, starting and ending at an intermediate facility. They considered a static problem where one aggregate, representative planning period is assumed.

In this paper, we study a variant of the LRP which can be defined as a Two-Echelon Capacitated Location Routing Problem with Split Deliveries (2E-CLRPSP). We further extend this problem with direct deliveries, and to tackle its complexity we propose three enhancements on an existing hybrid exact algorithm combining branch-and-bound and several local search structures. We apply our algorithm to find solutions for the expanding European supply chain for LNG as a fuel and gain interesting insights in this real-life network design problem.

2. Formal description and mathematical formulation

The network addressed in our problem consists of roadway edges $\mathcal{E}_r$, waterway edges $\mathcal{E}_w$, and a set of demand points $\mathcal{C}$ where customers take on LNG. We consider two types of facilities $\mathcal{F}$ from which LNG can be delivered to the demand points: import *terminals* (value of 1 in set $\mathcal{F}$) and *satellite* facilities (value of 2 in set $\mathcal{F}$). We define the sets $\mathcal{D}$ and $\mathcal{S}$ as the candidate locations for terminals and satellites, respectively. A candidate facility location can also be a demand point; hence, a single node in the network may belong to all three sets $\mathcal{D}$, $\mathcal{S}$ and $\mathcal{C}$. The problem is then defined on an undirected graph $\mathcal{G} = (\mathcal{V}, \mathcal{E})$, where $\mathcal{V} = \mathcal{D} \cup \mathcal{S} \cup \mathcal{C}$ and $\mathcal{E} = \mathcal{E}_r \cup \mathcal{E}_w$, considering a finite horizon T, where $\mathcal{T} = (1, 2, 3..., T)$, and the demand of node i is known for every period t and denoted by D_i^t.

Each type of facility $e \in \mathcal{F}$ at every candidate location $i \in \mathcal{D} \cup \mathcal{S}$ has an initial capacity B_i^e that can be expanded by investing in modular storage tanks with capacity C^e, up to a maximum capacity A_i^e. Moreover, a facility of type $e \in \mathcal{F}$ at location $i \in \mathcal{D} \cup \mathcal{S}$ has an initial construction cost F_i^e, an operating cost O_i^e (per m^3 of the total capacity) and an upgrade cost U_i^e. We define the set $\mathcal{M}_k$ as a set of vehicles for each type $k \in \mathcal{K}$. All the LNG that flows through the network can be transported by two types of vehicles $\mathcal{K}$: bunker barges (with a value of 1 in set $\mathcal{K}$) moving across waterway edges, and tanker trucks (with a value of 2 in $\mathcal{K}$) moving across roadway edges. Each type of vehicle $k \in \mathcal{K}$ has a maximum capacity G^k. Each facility has a dedicated fleet of vehicles. The maximum number of vehicles of type $k \in \mathcal{K}$ at location $i \in \mathcal{D} \cup \mathcal{S}$ for facility type $e \in \mathcal{F}$ is R_i^{ek}. Vehicles have an investment cost H^k, a fixed cost W^k when loading LNG at an import terminal, and a variable cost V^k per kilometer traveled.

The variables used to model the problem are as follows. Location decisions are modeled using binary variables γ_i^{et} equal to 1 if facility type e is located at node i in period t. Let ι_i^{et} indicate the capacity of facility type e installed at location i in period t, and ζ_i^{et} the number of upgrade modules installed at facility e at location i in period t. Routing decisions related to routes originated at terminals are modeled using binary variables α_{ijd}^{vkt}, which indicate whether a vehicle v of type k starting its trip from terminal d travels edge $(i,j) \in \mathcal{E}$ in period t. When a vehicle starts its trip from a satellite, the routing decisions are modeled with binary variables β_{ijs}^{vt}. Note that satellites can only be the start of the trip for tanker trucks, which means that the types of vehicles are not embedded into variables β. When a satellite is visited by a bunker barge, this barge had started its trip at a terminal. Delivery variables δ_{dj}^{vkt} indicate the volume of LNG delivered to customer $j \in \mathcal{C}$ from terminal d using vehicle v of type k in period t. Likewise, ϵ_{sj}^{vt} indicates the volume of LNG delivered to customer $j \in \mathcal{C}$ from satellite $s \in \mathcal{S}$ using vehicle v in period t. Note that in this problem we allow for split deliveries, which implies that a single customer may receive multiple deliveries from different facilities and different types of vehicles in a single period. Fleet size and mix decisions are modeled using variables κ_i^{ekt}, which represent the size of the fleet of vehicle type k at facility e at location i in period t. Finally, inventory is controlled using variables θ_s^t to measure the volume available at satellite s in period t. A graphical representation of the distribution network considered in this problem is shown in Figure 1.

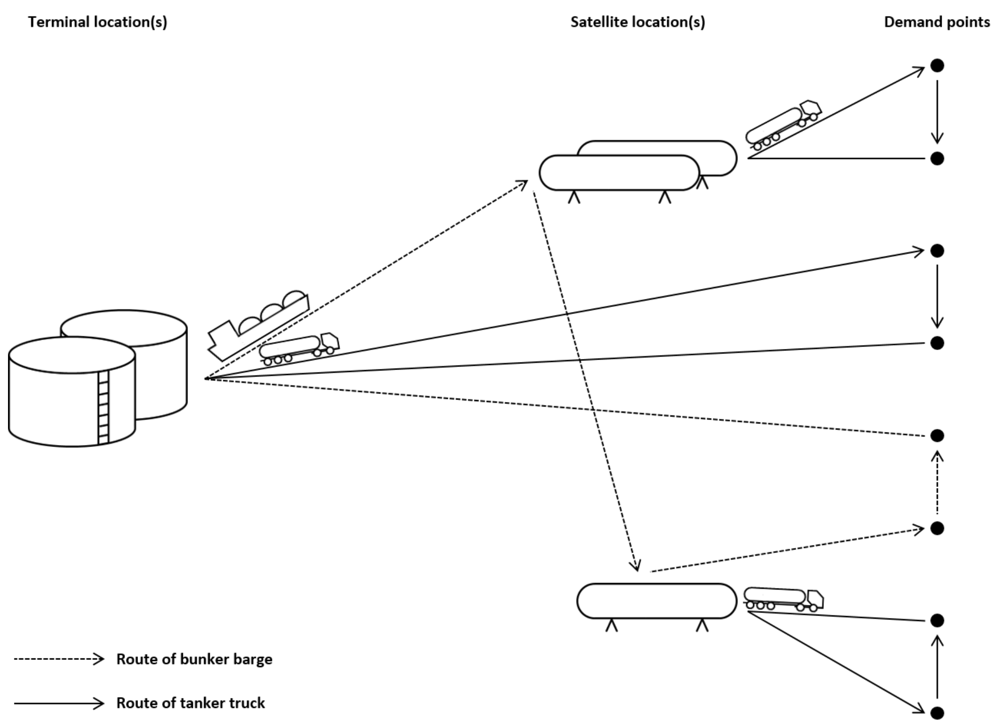

Figure 1: Graphical representation of the distribution network under consideration

We make the following assumptions: 1) Demand is assumed to be deterministic. Due to the early-stage development of the supply chain for LNG as a fuel, developers of new fuel stations or port locations often deploy contracts with customers to assure a certain demand volume per time period. Nevertheless, in real-world problems, demand will never be fully deterministic. In our case study design, we will therefore consider different demand volumes and geographical dispersion to incorporate various demand scenarios. 2) We assume that an import terminal is always fully replenished with LNG at the beginning of each period. This assumption is realistic because import terminals are very large and typically serve the supply chain for LNG as a fuel

Set	*Description*
$\mathcal{V}$	Nodes
$\mathcal{E}$	Edges
$\mathcal{E}_w$	Waterway edges
$\mathcal{E}_r$	Roadway edges
$\mathcal{C}$	Demand points
$\mathcal{D}$	Candidate terminal locations
$\mathcal{S}$	Candidate satellite locations
$\mathcal{F}$	Facility types (1 = terminal, 2 = satellite)
$\mathcal{K}$	Vehicle types (1 = bunker barges, 2 = tanker trucks)
$\mathcal{M}_k$	Set of vehicles of type $k \in \mathcal{K}$
$\mathcal{T}$	Set of periods
Parameter	*Description*
F_i^e	Opening cost of facility type $e \in \mathcal{F}$ at location $i \in \mathcal{D} \cup \mathcal{S}$
O_i^e	Operating cost of facility type $e \in \mathcal{F}$ at location $i \in \mathcal{D} \cup \mathcal{S}$
U_i^e	Unit upgrade cost of facility type $e \in \mathcal{F}$ at location $i \in \mathcal{D} \cup \mathcal{S}$
B_i^e	Initial capacity of facility type $e \in \mathcal{F}$ at location $i \in \mathcal{D} \cup \mathcal{S}$
C^e	Capacity of one module for upgrading facility type $e \in \mathcal{F}$
A_i^e	Maximum capacity of facility type $e \in \mathcal{F}$ at location $i \in \mathcal{D} \cup \mathcal{S}$
H^k	Investment cost of a vehicle of type $k \in \mathcal{K}$
W^k	Fixed cost of using a vehicle of type $k \in \mathcal{K}$
V^k	Variable cost of vehicle type $k \in \mathcal{K}$ per km
G^k	Capacity of vehicle type $k \in \mathcal{K}$
R_i^{ek}	Maximum number of vehicles of type $k \in \mathcal{K}$ at facility type $e \in \mathcal{F}$ at location $i \in \mathcal{D} \cup \mathcal{S}$
D_i^t	Demand at location $i \in \mathcal{C}$ in period $t \in \mathcal{T}$
L_{ij}^k	Distance between locations i and j for vehicle type $k \in \mathcal{K}$
T	Horizon
Variable	*Description*
γ_i^{et}	if facility type e is open at location i in period t
α_{ijd}^{vkt}	if vehicle v of type k starting from terminal d travels edge $(i,j) \in \mathcal{E}$ in period t
β_{ijs}^{vt}	if vehicle v (of type tanker truck) starting from satellite s travels edge $(i,j) \in \mathcal{E}_r$ in period t
δ_{dj}^{vkt}	volume delivered to j from terminal d using vehicle v of type k in period t
ϵ_{sj}^{vt}	volume delivered to j from satellite s using vehicle v in period t
μ_{ijd}^{vkt}	load of vehicle v of type k starting from terminal d traveling edge $(i,j) \in \mathcal{E}$ in period t
ν_{ijs}^{vt}	load of vehicle v starting from satellite s traveling edge $(i,j) \in \mathcal{E}$ in period t
ζ_i^{et}	number of module upgrades at facility type e at location i in period t
θ_i^t	inventory at satellite i in period t
ι_i^{et}	capacity of facility type e at location i in period t
κ_i^{ekt}	fleet size of vehicle type k of facility type e at location i in period t

with only a small part of their total capacity. 3) Any demand at nodes with an open terminal or satellite is fulfilled by that facility directly, without the need of a tanker truck or bunker barge. Most operating or scheduled terminals and satellites provide the option to also take on fuel by customers directly. 4) All the inventories in the satellites are to be replenished from the terminals. 5) Satellites can only be replenished by means of bunker barges, and can only deliver LNG to demand points by means of tanker trucks. This restriction is not driven by physical constraints (in principle a tanker truck could replenish a satellite), but rather by economic logic. If, for example, a tanker truck were to first replenish a satellite, and a demand point is satisfied by a tanker truck from that satellite, it would always be more cost-effective to simply replenish the demand point without the extra handling at the satellite. One implication of this assumption is that satellites can only be located at nodes that are connected to both waterway and roadway edges. Another implication is that lateral transshipment between satellites is not allowed.

The objective function is formulated in (1). Its first part minimizes the opening, upgrade and periodic operating costs of the facilities as well as the total investment costs associated with the fleet of vehicles. The second part minimizes the fixed cost associated with using the vehicles. The third part minimizes the variable routing costs of the vehicles.

$$
\begin{aligned}
&\text{minimize} \sum_{i \in \mathcal{D} \cup \mathcal{S}} \sum_{e \in \mathcal{F}} \left(\gamma_i^{eT} F_i^e + \zeta_i^{eT} U_i^e + \sum_{t \in \mathcal{T}} \iota_i^{et} O_i^e + \sum_{k \in \mathcal{K}} \kappa_i^{ekT} H^k \right) + \\
&\sum_{t \in \mathcal{T}} \sum_{j \in \mathcal{V}} \left(\sum_{k \in \mathcal{K}} \sum_{d \in \mathcal{D}} \sum_{v \in \mathcal{M}_k} \alpha_{djd}^{vkt} W^k + \sum_{s \in \mathcal{S}} \sum_{w \in \mathcal{M}_2} \beta_{sjs}^{wt} W^2 \right) + \\
&\sum_{t \in \mathcal{T}} \sum_{i \in \mathcal{V}} \sum_{j \in \mathcal{V}} \left(\sum_{k \in \mathcal{K}} \sum_{d \in \mathcal{D}} \sum_{v \in \mathcal{M}_k} \alpha_{ijd}^{vkt} L_{ij}^k V^k + \sum_{s \in \mathcal{S}} \sum_{w \in \mathcal{M}_2} \beta_{ijs}^{wt} L_{ij}^2 V^2 \right)
\end{aligned} \tag{1}
$$

Constraints (2)–(12) deal with the opening of facilities and the fulfillment of customer demand. Constraints (2) and (3) prevent terminals and satellites to be opened at nodes where they cannot be constructed. Constraints (4) imply that at most one of both facility types can be open at a node. Constraints (5) ensure that an open facility stays open for all future time periods. Constraints (6) ensure that a satellite is exclusively served by an LNG bunker ship, by prohibiting LNG tanker trucks, originating from either import terminals or other satellites, to deliver LNG to this facility. Constraints (7) guarantee that no deliveries of LNG are made to locations where a terminal is open. Constraints (8) and (9) ensure that deliveries of LNG can only be made from open facilities. Constraints (10) ensure that the demand of each customer is satisfied by means of a tanker truck or a bunker barge whenever there is no open terminal or satellite. Constraints (11) and (12) ensure that vehicle capacities are respected.

$$\gamma_i^{1t} = 0 \qquad i \in \mathcal{V} \setminus \mathcal{D}, t \in \mathcal{T} \tag{2}$$

$$\gamma_i^{2t} = 0 \qquad i \in \mathcal{V} \setminus \mathcal{S}, t \in \mathcal{T} \tag{3}$$

$$\gamma_i^{1t} + \gamma_i^{2t} \leq 1 \qquad i \in \mathcal{D} \cup \mathcal{S}, t \in \mathcal{T} \tag{4}$$

$$\gamma_i^{et} \geq \gamma_i^{et-1} \qquad i \in \mathcal{D} \cup \mathcal{S}, e \in \mathcal{F}, t \in \mathcal{T} \setminus 1 \tag{5}$$

$$\sum_{v \in \mathcal{M}_2} \left(\sum_{d \in \mathcal{D}} \delta_{ds}^{v2t} + \sum_{i \in \mathcal{S}} \epsilon_{is}^{vt} \right) \leq \left(1 - \gamma_s^{2t}\right) G^2 \qquad s \in \mathcal{S}, t \in \mathcal{T} \tag{6}$$

$$\sum_{k\in\mathcal{K}}\sum_{v\in\mathcal{M}_k}\sum_{u\in\mathcal{D}}\delta_{ud}^{vkt}+\sum_{s\in\mathcal{S}}\epsilon_{sd}^{vt}\le\left(1-\gamma_d^{1t}\right)G^1 \qquad d\in\mathcal{D},t\in\mathcal{T} \tag{7}$$

$$\sum_{k\in\mathcal{K}}\sum_{v\in\mathcal{M}_k}\sum_{j\in\mathcal{C}\cup\mathcal{S}}\delta_{dj}^{vkt}\le\gamma_d^{1t}A_d^1 \qquad d\in\mathcal{D},t\in\mathcal{T} \tag{8}$$

$$\sum_{v\in\mathcal{M}_2}\sum_{j\in\mathcal{C}}\epsilon_{sj}^{vt}\le\gamma_s^{2t}A_d^2 \qquad s\in\mathcal{S},t\in\mathcal{T} \tag{9}$$

$$\sum_{d\in\mathcal{D}}\sum_{k\in\mathcal{K}}\sum_{v\in\mathcal{M}_k}\delta_{dj}^{vkt}+\sum_{s\in\mathcal{S}}\sum_{w\in\mathcal{M}_2}\epsilon_{sj}^{wt}\ge\left(1-\sum_{e\in\mathcal{F}}\gamma_j^{et}\right)D_j^t \qquad j\in\mathcal{C},t\in\mathcal{T} \tag{10}$$

$$\sum_{j\in\mathcal{C}\cup\mathcal{S}}\delta_{dj}^{vkt}\le G^k \qquad d\in\mathcal{D},v\in\mathcal{M}_k,k\in\mathcal{K},t\in\mathcal{T} \tag{11}$$

$$\sum_{j\in\mathcal{C}}\epsilon_{sj}^{vt}\le G^2 \qquad d\in\mathcal{S},v\in\mathcal{M}_2,t\in\mathcal{T} \tag{12}$$

Constraints (13)–(19) control the facility inventory and capacity. Constraints (13) ensure that the inventory level of a satellite is zero when the satellite is not open. Constraints (14) keep track of the inventory level of the satellites at the end of every period. In these constraints, we incorporated incoming deliveries of LNG from other satellites (even though lateral transshipment is not allowed) because we need to ensure that the constraint is also valid when no satellite is built at the location. Similarly, we included the term $(1-\gamma_s^{1t})$ in order to guarantee that the constraints are valid in case a terminal is built at the location. Constraints (15) and (16) ensure the capacity of the facilities is not exceeded. Constraints (17) bound the capacity of the facilities while constraints (18) track and update the facility sizes. Constraints (19) ensure that the capacity of the facilities is not downgraded.

$$\gamma_s^{2t}\mathcal{A}_s^2\ge\theta_s^t \qquad s\in\mathcal{S},t\in\mathcal{T} \tag{13}$$

$$\theta_s^{t-1}+\sum_{d\in\mathcal{D}}\sum_{k\in\mathcal{K}}\sum_{v\in\mathcal{M}_k}\delta_{ds}^{vkt}+\sum_{w\in\mathcal{M}_2}\left(\sum_{u\in\mathcal{S}}\epsilon_{us}^{wt}-\sum_{j\in\mathcal{C}}\epsilon_{sj}^{wt}\right)-\left(1-\gamma_s^{1t}\right)D_s^t=\theta_s^t \qquad s\in\mathcal{S},t\in\mathcal{T} \tag{14}$$

$$\theta_s^{t-1}+\sum_{d\in\mathcal{D}}\sum_{k\in\mathcal{K}}\sum_{v\in\mathcal{M}_k}\delta_{ds}^{vkt}-\left(1-\sum_{e\in\mathcal{F}}\gamma_s^{et}\right)D_s^t\le\iota_s^{2t} \qquad s\in\mathcal{S},t\in\mathcal{T} \tag{15}$$

$$\sum_{k\in\mathcal{K}}\sum_{v\in\mathcal{M}_k}\sum_{j\in\mathcal{C}\cup\mathcal{S}}\delta_{dj}^{vkt}+\gamma_d^{1t}D_d^t\le\iota_d^{1t} \qquad d\in\mathcal{D},t\in\mathcal{T} \tag{16}$$

$$\gamma_i^{et}A_i^e\ge\iota_i^{et} \qquad i\in\mathcal{D}\cup\mathcal{S},e\in\mathcal{F},t\in\mathcal{T} \tag{17}$$

$$\gamma_i^{et}B^e+\zeta_i^{et}C^e=\iota_i^{et} \qquad i\in\mathcal{D}\cup\mathcal{S},e\in\mathcal{F},t\in\mathcal{T} \tag{18}$$

$$\zeta_i^{et}\ge\zeta_i^{e,t-1} \qquad i\in\mathcal{D}\cup\mathcal{S},e\in\mathcal{F},t\in\mathcal{T}\setminus 1 \tag{19}$$

Constraints (20) and (21) control the fleet of vehicles available at each facility. Constraints (20) guarantee that the maximum number of vehicles allowed at a single location is not exceeded. Constraints (21) ensure that the number of vehicles at each location cannot be downgraded.

$$R_i^{ek}\ge\kappa_i^{ekt} \qquad i\in\mathcal{D}\cup\mathcal{S},e\in\mathcal{F},k\in\mathcal{K},t\in\mathcal{T} \tag{20}$$

$$\kappa_i^{ekt}\ge\kappa_i^{ekt-1} \qquad i\in\mathcal{D}\cup\mathcal{S},e\in\mathcal{F},k\in\mathcal{K},t\in\mathcal{T} \tag{21}$$

Constraints (22)–(35) manage the routing part of the problem. Constraints (22) ensure that a delivery of LNG from terminals to any node can only be made if that specific node is visited in the route. Constraints (23) ensure that every route starts at its corresponding terminal and constraints (24) ensure the route flow. Constraints (25) and (26) impose a limit of at most one outgoing and one incoming edge per vehicle in a node. Constraints (27) prevent using more vehicles than there are available in the fleet. Constraints (28)–(33) act in a similar way for the satellites. Constraints (34) and (35) avoid that tanker trucks travel over waterways and bunker barges over roadways.

$$\sum_{j\in\mathcal{V}} \alpha_{jid}^{vkt} G^k \geq \delta_{di}^{vkt} \qquad d\in\mathcal{D}, i\in\mathcal{C}\cup\mathcal{S}, v\in\mathcal{M}_k, k\in\mathcal{K}, t\in\mathcal{T} \tag{22}$$

$$\sum_{j\in\mathcal{V}} \alpha_{djd}^{vkt} G^k \geq \sum_{j\in\mathcal{V}} \delta_{dj}^{vkt} \qquad d\in\mathcal{D}, v\in\mathcal{M}_k, k\in\mathcal{K}, t\in\mathcal{T} \tag{23}$$

$$\sum_{j\in\mathcal{V}} \left(\alpha_{ijd}^{vkt} - \alpha_{jid}^{vkt}\right) = 0 \qquad d\in\mathcal{D}, i\in\mathcal{V}, v\in\mathcal{M}_k, k\in\mathcal{K}, t\in\mathcal{T} \tag{24}$$

$$\sum_{j\in\mathcal{V}} \alpha_{ijd}^{vkt} \leq 1 \qquad d\in\mathcal{D}, i\in\mathcal{V}, v\in\mathcal{M}_k, k\in\mathcal{K}, t\in\mathcal{T} \tag{25}$$

$$\sum_{j\in\mathcal{V}} \alpha_{jid}^{vkt} \leq 1 \qquad d\in\mathcal{D}, i\in\mathcal{V}, v\in\mathcal{M}_k, k\in\mathcal{K}, t\in\mathcal{T} \tag{26}$$

$$\sum_{j\in\mathcal{V}} \sum_{v\in\mathcal{M}_k} \alpha_{djd}^{vkt} \leq \kappa_d^{1kt} \qquad d\in\mathcal{D}, k\in\mathcal{K}, t\in\mathcal{T} \tag{27}$$

$$\sum_{j\in\mathcal{V}} \beta_{sjs}^{vt} G^2 \geq \sum_{j\in\mathcal{V}} \epsilon_{sj}^{vt} \qquad s\in\mathcal{S}, v\in\mathcal{M}_2, t\in\mathcal{T} \tag{28}$$

$$\sum_{j\in\mathcal{V}} \beta_{jis}^{vt} G^2 \geq \epsilon_{si}^{vt} \qquad s\in\mathcal{S}, i\in\mathcal{C}, v\in\mathcal{M}_2, , t\in\mathcal{T} \tag{29}$$

$$\sum_{j\in\mathcal{V}} \left(\beta_{ijs}^{vt} - \beta_{jis}^{vt}\right) = 0 \qquad s\in\mathcal{S}, i\in\mathcal{V}, v\in\mathcal{M}_2, t\in\mathcal{T} \tag{30}$$

$$\sum_{j\in\mathcal{V}} \beta_{ijs}^{vt} \leq 1 \qquad s\in\mathcal{S}, i\in\mathcal{V}, v\in\mathcal{M}_2, t\in\mathcal{T} \tag{31}$$

$$\sum_{j\in\mathcal{V}} \beta_{jis}^{vt} \leq 1 \qquad s\in\mathcal{S}, i\in\mathcal{V}, v\in\mathcal{M}_2, t\in\mathcal{T} \tag{32}$$

$$\sum_{j\in\mathcal{V}} \sum_{v\in\mathcal{M}_2} \beta_{sjs}^{vt} \leq \kappa_s^{22t} \qquad s\in\mathcal{S}, t\in\mathcal{T} \tag{33}$$

$$\sum_{v\in\mathcal{M}_1} \sum_{t\in\mathcal{T}} \sum_{d\in\mathcal{D}} \alpha_{ijd}^{v1t} = 0 \qquad \{i,j\in\mathcal{V} | (i,j)\notin\mathcal{E}_w\} \tag{34}$$

$$\sum_{v\in\mathcal{M}_2} \sum_{t\in\mathcal{T}} \left(\sum_{d\in\mathcal{D}} \alpha_{ijd}^{v2t} + \sum_{s\in\mathcal{S}} \beta_{ijs}^{vt} \right) = 0 \qquad \{i,j\in\mathcal{V} | (i,j)\notin\mathcal{E}_r\} \tag{35}$$

Subtours in the routes of both types of vehicles are eliminated using commodity flow constraints (36)–(43) based on [17]. Two new decision variables are introduced: μ_{ijd}^{vkt} and ν_{ijs}^{vt}, which represent the load of LNG on vehicle v of type k traversing edge (i,j) in period t when the route originates at a terminal or a satellite, respectively. Constraints (36) ensure that all the demand allocated to a terminal leaves the facility and constraints (37) ensure that the volume of LNG decreases after a demand location is satisfied. Constraints (38) impose that a vehicle returns to its terminal with no LNG and constraints (39) ensure that the flows of commodity only occur in edges visited in the route. Constraints (40)–(42) are similar for the fleet serving satellites only.

$$\sum_{d\in\mathcal{D}}\sum_{j\in\mathcal{V}}\sum_{v\in\mathcal{M}_k}\sum_{k\in\mathcal{K}}\mu_{djd}^{vkt} = \sum_{d\in\mathcal{D}}\sum_{j\in\mathcal{V}}\sum_{v\in\mathcal{M}_k}\sum_{k\in\mathcal{K}}\delta_{dj}^{vkt} \qquad t\in\mathcal{T} \tag{36}$$

$$\sum_{j\in\mathcal{V}}\mu_{jid}^{vkt} - \sum_{j\in\mathcal{V}}\mu_{ijd}^{vkt} = \delta_{di}^{vkt} \qquad d\in\mathcal{D}, i\in\mathcal{V}\setminus d, v\in\mathcal{M}_k, k\in\mathcal{K}, t\in\mathcal{T} \tag{37}$$

$$\mu_{idd}^{vkt} = 0 \qquad d\in\mathcal{D}, i\in\mathcal{V}, v\in\mathcal{M}_k, k\in\mathcal{K}, t\in\mathcal{T} \tag{38}$$

$$\sum_{j\in\mathcal{V}}\alpha_{jid}^{vkt}G^k \geq \sum_{j\in\mathcal{V}}\mu_{jid}^{vkt} \qquad d\in\mathcal{D}, i\in\mathcal{V}, v\in\mathcal{M}_k, k\in\mathcal{K}, t\in\mathcal{T} \tag{39}$$

$$\sum_{s\in\mathcal{S}}\sum_{j\in\mathcal{V}}\sum_{v\in\mathcal{M}_2}\nu_{sjs}^{vt} = \sum_{s\in\mathcal{S}}\sum_{j\in\mathcal{V}}\sum_{v\in\mathcal{M}_2}\epsilon_{sj}^{vt} \qquad t\in\mathcal{T} \tag{40}$$

$$\sum_{j\in\mathcal{V}}\nu_{jis}^{vt} - \sum_{j\in\mathcal{V}}\nu_{ijs}^{vt} = \epsilon_{si}^{vt} \qquad s\in\mathcal{S}, i\in\mathcal{V}\setminus s, v\in\mathcal{M}_2, t\in\mathcal{T} \tag{41}$$

$$\nu_{iss}^{vt} = 0 \qquad s\in\mathcal{S}, i\in\mathcal{V}, v\in\mathcal{M}_2, t\in\mathcal{T} \tag{42}$$

$$\sum_{j\in\mathcal{V}}\beta_{jis}^{vt}G^2 \geq \sum_{j\in\mathcal{V}}\nu_{jis}^{vt} \qquad s\in\mathcal{S}, i\in\mathcal{V}, v\in\mathcal{M}_2, t\in\mathcal{T} \tag{43}$$

The formulation of the model can be further tightened by adding constraints (44) and (45), which break symmetry for the routes of both types of vehicles.

$$\sum_{d\in\mathcal{D}}\sum_{i\in\mathcal{C}\cup\mathcal{S}}\left(\delta_{di}^{vkt} - \delta_{di}^{v-1kt}\right) \leq 0 \qquad v\in\mathcal{M}_k\setminus 1, k\in\mathcal{K}, t\in\mathcal{T} \tag{44}$$

$$\sum_{s\in\mathcal{S}}\sum_{i\in\mathcal{C}}\left(\epsilon_{si}^{vt} - \epsilon_{si}^{v-1t}\right) \leq 0 \qquad v\in\mathcal{M}_2\setminus 1, t\in\mathcal{T} \tag{45}$$

Constraints (46)–(48) define the domain of the decision variables.

$$\alpha_{ijd}^{vkt}, \beta_{ijs}^{vt}, \gamma_{ie}^{t} \in \{0,1\} \tag{46}$$

$$\delta_{ij}^{vkt}, \epsilon_{ij}^{vt}, \iota_{ie}^{t}, \theta_i^t, \mu_{ijd}^{vkt}, \nu_{ijd}^{vkt} \geq 0 \tag{47}$$

$$\zeta_{ie}^{t}, \kappa_{ek}^{t} \in \mathbb{Z}^+ \tag{48}$$

3. Solution algorithm

In this section we describe the algorithm used to solve the problem and several improvements we have made to it. This algorithm is inspired by the variable MIP neighborhood descent (VMND) of Larrain et al. [19]. The algorithm is described in Section 3.1, after which improvement opportunities are described in Section 3.2. In Section 3.3, we show how to apply this algorithm to the problem at hand.

3.1. Description of the variable MIP neighborhood descent algorithm

VMND was introduced to solve an inventory management and vehicle routing problem arising in the cash logistics industry, and is based on formulating the problem as a MIP, which is then solved with several heuristic rules, such as in a fix-and-optimize framework. Such a structure allows for quickly obtaining upper bounds, while still retaining the information of the lower bound, thus being able to prove optimality and/or to compute the gap of a solution. Hence, VMND is an exact algorithm, which alternates between two phases, a local search phase and an exact phase.

During the local search phase, the main problem is restricted by new constraints, i.e., performing a local search similar to a Variable Neighborhood Search (VNS) [23]. Different neighborhoods are explored using the best improvement heuristic. The solution of the best improvement is given back to the exact phase as a starting solution, which significantly increases the performance of the exact phase. Moreover, the exact phase is limited by the amount of time that the algorithm spends in the local search phase. The algorithm switches back to the local search phase when a new solution is found, or the time limit has been exceeded.

3.2. Improvement opportunities

Figure 2 visualizes the new algorithm. Three opportunities have been identified that can increase the performance of the VMND algorithm proposed by Larrain et al. [19]. The first one relates to the number of times the algorithm alternates between the two phases. Initially, the VMND algorithm was designed to switch from the local search phase to the exact phase when an improved solution is found in a neighborhood or when the largest neighborhood has been exhausted. This entails invoking the exact phase several times, which can be beneficial for small problems for which the exact phase is easy and not very time-consuming. However, when the size of the problem increases due to a larger number of demand points, vehicles, or candidate facility locations, the model size increases and the exact phase will take significantly longer. Therefore, a first improvement is to change neighborhoods similar to a Basic VNS as described in Duarte et al. [11]. This will decrease the number of alternations while improving the best found solution. The benefit will also come from the reduced time spent in the exact phase.

A second improvement opportunity resides in ensuring that the exact phase only switches back to the local search phase when a new solution has been found. This can be beneficial because it prevents the algorithm from switching back to the local phase when the optimal upper bound is reached, but an optimality gap still exists. In addition, new solutions obtained form the exact phase are needed in order to prevent the algorithm from getting stocked in local optimal solutions.

The third improvement opportunity is to decrease the amount of redundant time spent exploring the neighborhoods. During the exploration of neighborhoods, a significant proportion of computing time can be devoted to decreasing the relative MIP gap from, say, 2% to 0%. It can be observed empirically, however, that there is little to no added value for the last explorations when no improvement is found. For this reason, two new parameters have been added to the algorithm which cut off the exploration of neighborhoods. The first parameter is a time limit ϕ and the second one is a relative MIP gap tolerance for exploring neighborhoods, denoted as λ.

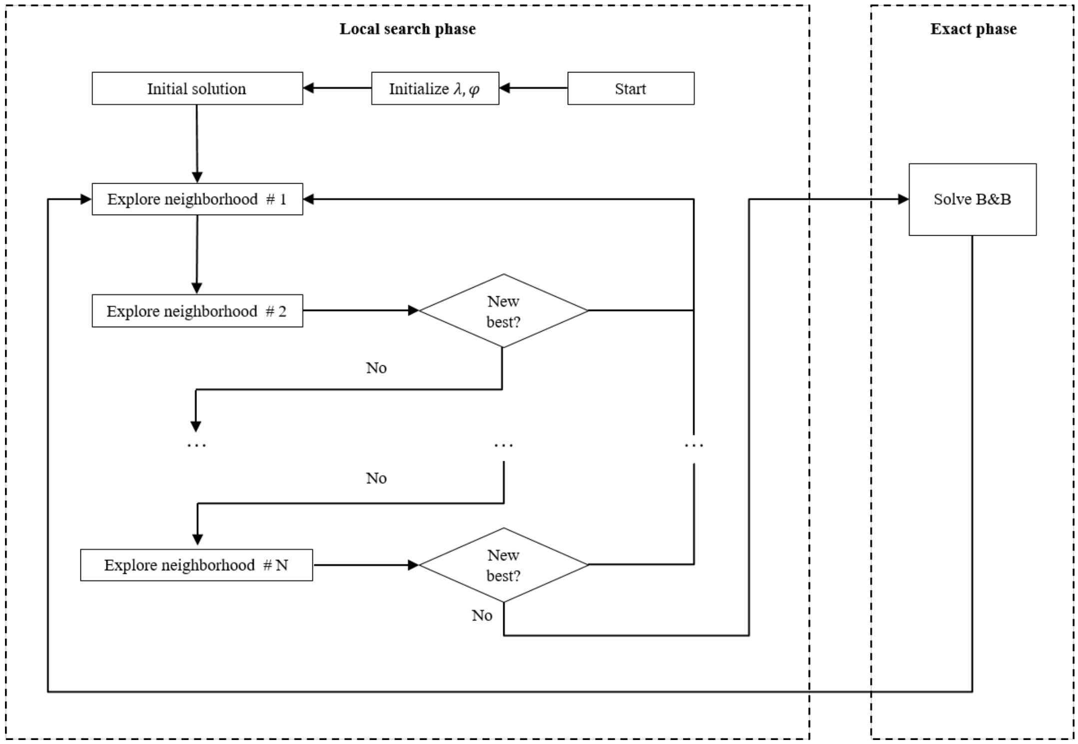

Figure 2: Improved VMND algorithm

3.3. *Applying the improved VMND to the 2E-CLRPSP*

We have designed four neighborhoods based on the structure of the problem. These are meant to allow the algorithm to change all decisions variables while not yielding too difficult MIPs. The neighborhoods together with their defining operations are:

1. *Route:* changing one route of one vehicle in one time period. This neighborhood fixes the routes of all vehicles except one, and iterates over all vehicles and periods.
2. *Vehicles:* changing the routes of one specific vehicle across all periods. Here, we allow one vehicle to be kept free over all the planning horizon, while the routes of all other vehicles are fixed.
3. *Periods:* changing all variables in two periods. We take every pair of periods and let all their associated variables be free.
4. *Satellites:* changing one terminal and two satellites across all periods. Here, we allow more flexibility by exploring the interactions among three facilities, being one terminal and a pair of satellites.

Table 1: Neighborhood definitions

n	Neighborhood	$\mathcal{P}_n$	p	MIP size
1	Route	$\mathcal{M} \times \mathcal{K} \times \mathcal{T}$	(v_p, k_p, t_p)	E
2	Vehicles	$\mathcal{M} \times \mathcal{K}$	(v_p, k_p)	ET
3	Periods	$\mathcal{T}$	$(t1_p, t2_p)$	$2EKSM$
4	Satellites	$\mathcal{D} \times (\mathcal{S} \times \mathcal{S}_{-1})/2$	$(d_p, s1_p, s2_p)$	$2EKTM$

Table 1 describes the neighborhoods and their characteristics. A neighborhood is defined as the solutions that can be reached by applying an operator to a given solution. Every neighborhood $n \in \mathcal{V}$ has an associated set of valid parameterizations $\mathcal{P}_n$. A parametrized neighborhood is denoted as n_p with parameters $p \in \mathcal{P}_n$. In this table, E represents the number of edges, T the number of time periods, K the number of different types of vehicles, M the number of vehicles and S the number of candidate satellite locations. One parametrization of neighborhood "Route" could be $v = 2$, $k = 1$ and $t = 3$, which allows the model to change the route of the second bunker barge (vehicle type $k = 1$) in the third time period. All other routes are fixed in the current solution.

The developed neighborhoods differ in size and complexity. In order to provide an estimate of the complexity of the subproblem, the MIP size is given. The MIP size is the upper bound to the number of free variables per individual decision variable in a neighborhood. The complexity of a neighborhood can be calculated by multiplying the MIP size by the number of possible combinations $\mathcal{P}_n$ in the neighborhood.

Each neighborhood can be seen as a new subproblem that results in a local optimal solution when solved. Neighborhoods "Route" and "Vehicles" can be defined as LRPs with one vehicle and semi-fixed facilities; "Periods" as a 2E-LRP with two periods; "Satellites" as a 2E-LRP with one terminal and two satellites. Facilities are said to be semi-fixed, as the decision variable γ handling the opening of facilities is free. However, when routing variables are fixed, the facilities that are part of the route must be open. Table 2 shows the fixed variables for each neighborhood.

Table 2: Fixed values in neighborhoods

Variable	Route	Vehicles	Periods	Satellites
α_{ijd}^{vkt}	$t \neq t_p$ $k \neq k_p$ $v \neq v_p$	$k \neq k_p$ $v \neq v_p$	$t \neq t_p$	Free
β_{ijs}^{vt}	$t \neq t_p$ $k \neq k_p$ $v \neq v_p$	$k \neq k_p$ $v \neq v_p$	$t \neq t_p$	Free
γ_i^{et}	Free	Free	Free	$i \neq i_p$ $e \neq 2$
δ_{dj}^{vkt}	$t \neq t_p$ $k \neq k_p$ $v \neq v_p$	$k \neq k_p$ $v \neq v_p$	$t \neq t_p$	Free
ϵ_{sj}^{vt}	$t \neq t_p$ $k \neq k_p$ $v \neq v_p$	$k \neq k_p$ $v \neq v_p$	$t \neq t_p$	Free
ζ_i^{et}	Free	Free	Free	Free
θ_i^t	Free	Free	Free	Free
ι_i^{et}	Free	Free	Free	Free
κ^{ekt}	Free	Free	Free	Free

4. Computational experiments

In this section, we present the computational experiments. In Section 4.1, we describe the experimental design used to evaluate our algorithm. In Section 4.2, we show the results of a detailed sensitivity analysis performed on the parameters and neighborhoods of our algorithm to determine the best combination of parameter values. In Section 4.3 we assess the performance of our algorithm against the original VMND algorithm of Larrain et al. [19] and against CPLEX.

4.1. Experimental design

We have generated 26 instances by varying the number of candidate terminal locations (D), candidate satellite locations (S), demand points (C), and time periods (T). An instance is then characterized by its configuration $D/S/C/T$. The demand at each customer node was generated using a uniform distribution. For nodes that can be accessed exclusively through roadway edges, the demand was generated using the range $[100, 200]$; the demand for locations that can be accessed by both types of edges was generated using the range $[150, 250]$. All approaches were coded in Java and we used CPLEX 12.8 as a MIP solver. Unless otherwise specified, all tests were executed with a time limit of 3 hours and a memory limit of 30GB. The experiments are carried out on an Intel Xeon E5 2680v3 CPU (2.5GHz) with 40GB memory. We allow CPLEX to use up to 4 threads in every execution.

4.2. Sensitivity analysis on the time limit and optimality gap parameters of the local search

We evaluated the performance of the algorithm with respect to the time limit ϕ put on solving the subproblems arising in the local search, and with respect to the optimality gap λ that must be achieved before the problem is deemed solved. We define a default case, which allows each subproblem to be solved for up to 1000 seconds, or when optimality has been proven at a 0.00% gap. We select a subset of 10 test instances with a different size and vary the time limit ϕ and the relative gap tolerance λ to guide how to order the neighborhoods and to define suitable values for those parameters.

4.2.1. Time limit ϕ

In order to test the influence of the time limit parameters, three different input values are given for ϕ: 10, 20 and 50 seconds. Table 3 shows the decrease in computing time for the different input values. A positive value reflects a decrease in computing time compared to the default case, while a negative value points to an increase in computation time.

Table 3: Average decrease in computing times compared to the default case $\phi = 1000$s

ϕ	Route	Vehicles	Periods	Satellites	Average
10s	16.82%	5.81%	-9.94%	55.42%	17.03%
20s	3.89%	4.68%	-3.63%	5.25%	2.55%
50s	-1.10%	4.67%	3.97%	-6.56%	0.25%

The quality of the results depicted in Table 3 show a high dependency on the complexity of the newly created subproblem. The smaller and less complex neighborhoods “Route”, “Vehicles” and “Periods” show little impact on their behavior. This is due to the low complexity of the problem and the relatively high time limit for these specific neighborhoods. The time limit is only exceeded in the last iteration of the local search phase for these relatively small problems. A greater impact is seen in the more complex neighborhood “Satellites”. The local search phase is then truncated. This can lead to less redundant computations and therefore increase performance.

The influence of the time limit can also be observed in the behavior of the solution over time. Figure 3a shows two typical behaviors related to a low time limit, applied to a typical instance. The first phenomenon that can be observed is that a low time limit can negatively influence the neighborhoods' ability to quickly decrease the objective value. This can result in fewer new solutions and a higher upper bound in the local search phase, and can potentially lead to longer computing times in the exact phase. The second phenomenon shows that a low time limit can be beneficial. After some time, the low time limit can outperform the default case. The local search takes longer as the relative gap in the exact phase is becoming smaller. Therefore, the time limit will mainly cut the local search later in the algorithm. A similar behavior is observed for another neighborhood in Figure 3b.

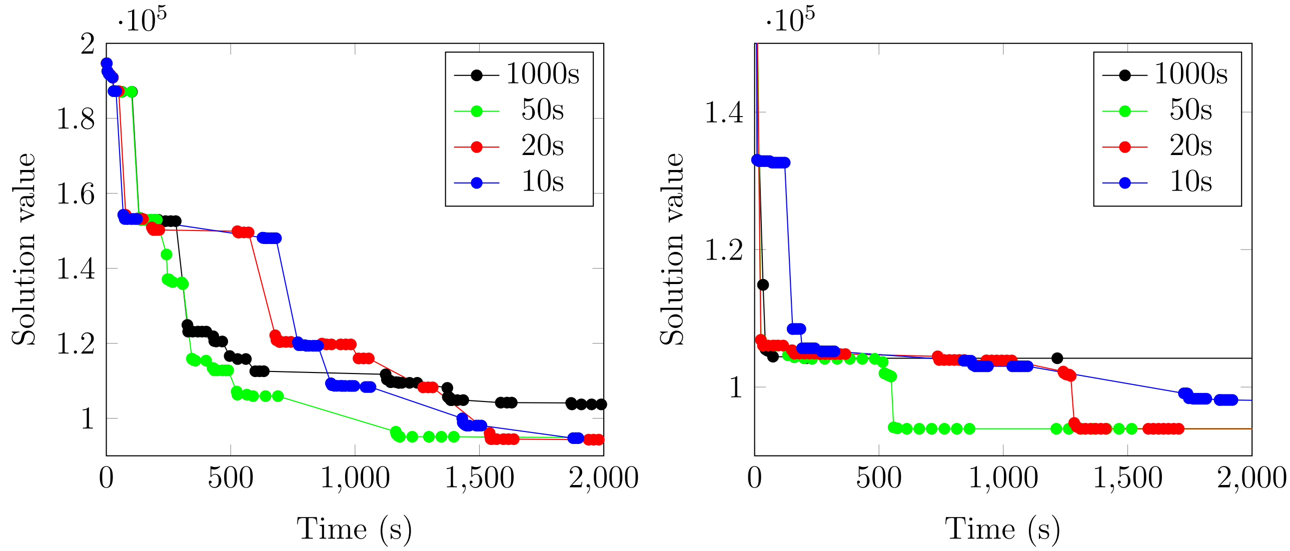

(a) Neighborhood "Periods"

(b) Neighborhood "Satellites"

Figure 3: The behavior related to the time limit ϕ of two neighborhoods in instance 26

The test results show that it can be beneficial to lower the time limit such that long neighborhood explorations are eliminated. As the complexity of each neighborhood varies, setting a low time limit can help finish the execution of a more complex neighborhood, while it will have no effect in a smaller neighborhood. The time limit can be used in such a way that it operates as an upper bound of the largest neighborhood.

4.2.2. Relative gap tolerance λ

The relative gap tolerance limit λ restricts the exploration of a neighborhood up until the set value. The influence of this limit is tested on four values of λ: 2%, 5%, 10% and 20%. Table 4 shows the decrease in computing times for the subset of tested instances.

The lowest value of λ results in the worst average performance and decreases the average computing time by 37.35% when compared to the default case. The best average performance is achieved when setting the relative gap limit to 10%. This decreases the average running times by 59.36% and consistently decreases running times in all neighborhoods by more than 40%. The lower performance of the lowest value for the gap tolerance limit is due to longer computing times in the local search phase. A higher value of λ can also result in decreased performance.

Table 4: The decrease in computing times compared to $\lambda = 0\%$

Value of λ	Route	Vehicles	Periods	Satellites	Average
0.02	61.86%	37.41%	33.54%	16.59%	37.35%
0.05	72.85%	52.95%	42.56%	60.24%	57.15%
0.10	53.86%	57.86%	43.67%	82.06%	59.36%
0.20	56.97%	57.90%	43.31%	15.30%	43.37%

This happens when the gap tolerance is too high and does not allow the neighborhood to converge and find new solutions.

Figure 4 shows the behavior of neighborhoods "Satellites" and "Periods" applied to a typical instance. It can be seen from Figure 4b that most variations outperform the default case. The long and extensive local searches are cut off which allows the exact phase to find a new better solution. Figure 4a shows a behavior in which the lowest value is the weakest performer, after the default case. In this case, the lower quality solutions given to the exact phase result in a weaker performance of that phase.

The test results show that the relative gap tolerance limit can eliminate excessive neighborhood exploration and considerably increase performance. It must be chosen in such a way that it is not so low that it would not exhaust neighborhoods and not so high that valuable information would be lost.

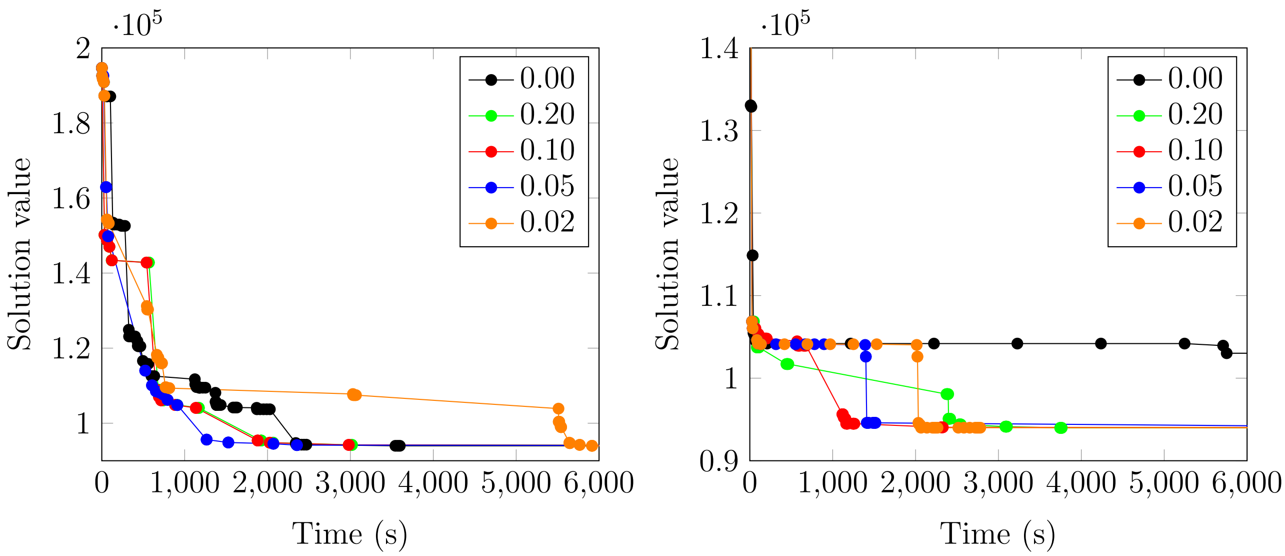

(a) Neighborhood "Periods"

(b) Neighborhood "Satellites"

Figure 4: The behavior related to the time limit λ of two neighborhoods in instance 26

4.3. Computational results

We solved 26 instances using CPLEX 12.8, the original algorithm proposed by Larrain et al. [19] and the improved algorithm proposed in this paper. The sequence of the neighborhoods is based on the results of Sections 4.2.1 and 4.2.2 and on increasing neighborhood complexity. We used the same sequence of neighborhoods for the implementation of the VMND Larrain et al. [19] and the improved VMND.

Table 5 shows the results of all 26 instances for the three approaches. For each approach, we report the upper bound, the relative gap and the wall time (s). In those cases where the execution of an instance is stopped because the memory limit was exceeded, an asterisk is placed next to the running time.

The results show that from the 26 instances, 8 instances were solved to optimality for at least one of the three approaches; all these instances have a planning horizon of two periods, which is the shortest considered in this study. All three approaches solved 6 of these instances to optimality (i.e., instances 10, 18-21, 23). The improved algorithm was the only approach that solved instance 11 to optimality within the allowed time frame, but it was also the only one that did not close the gap for instance 22. From those 6 instances that were solved to optimality for all three approaches, the average wall time was 58.8 seconds for CPLEX, 160 seconds for the VMND and 80 seconds for the improved algorithm. This result is intuitive given that for relatively small and easy instances, CPLEX can obtain the optimal solution very fast without the help of a local search heuristic.

Considering only the 18 instances that were not solved to optimality by any of the approaches, the average gap was 4.3% for the CPLEX model, 3.7% for the VMND and 2.7% for the improved algorithm. For 13 of these instances the improved algorithm had the lowest gap of all approaches (e.g., instances 6, 14) while it was outperformed by either CPLEX and/or the original VMND for only three instances (i.e., instances 1, 9, 12). In instances 15 and 17, which are among the largest instances considered in this study, the improved algorithm performed notably good against the other approaches. In both instances the gap difference between the improved algorithm and CPLEX and the VMND was 13.2% and 10.6% respectively. These results suggest that the improved algorithm performs better than the other two approaches on relatively large instances that cannot be solved within the time limit.

Regarding the upper bound, all three approaches obtained the same upper bound for the majority of instances. In total, CPLEX obtained the best upper bound for 20 instances, while the VMND and the improved algorithm obtained the best upper bound for 23 and 25 instances, respectively. Although we observe no major difference among the approaches in this regard, during the computational experiments we did observe that the improved algorithm obtained better upper bounds faster than the other two approaches, which helped the B&B procedure to prune more branches in the early stages of the exact phase and, hence, achieve a lower gap than the other two approaches at the moment where the time limit was reached.

5. Case study

We apply our algorithm to gain insights into how best to expand the supply chain for LNG as a fuel in Europe. The Alternative Fuels Directive 2014/94/EU specifies that Member States of the European Union should ensure the availability of alternative fuels, such as LNG, at least along the TEN-T Core Network by the end of 2030. In this case study, we focus our analyses on a part of the TEN-T Core Network that is connected to the LNG import terminal at the Port of Rotterdam (see Figure 5). The network includes 18 nodes where demand for LNG as a fuel is starting to develop. Those nodes are connected by means of four of the TEN-T corridors. Some nodes are connected by roadway and waterway, others only by roadway. Our case study design is aimed at gaining insight into the conditions under which one or more satellites will be opened. To this end, three candidate satellite locations are considered, with each one located

Table 5: Results of the computational experiments for all three approaches. An asterisk next to the wall time indicates that execution of the approach was stopped because the memory limit was exceeded

		CPLEX			VMND			Improved VMND		
#	Scenario	U bound	Gap (%)	Time (s)	U bound	Gap (%)	Time (s)	U bound	Gap (%)	Time (s)
1	2/2/2/2	78760	0.2	10800	78760	0.2	10800	78760	0.3	*6454
2	2/2/2/4	87660	0.7	10800	87660	0.7	10800	87660	0.7	*7559
3	2/2/2/6	96180	0.8	*5465	96180	0.7	10800	96180	0.7	10801
4	2/2/6/2	94570	0.7	*8938	94570	0.6	10800	94570	0.6	10801
5	2/2/6/4	109390	1.8	10800	109390	1.5	10800	109390	1.5	10801
6	2/2/6/6	125390	6.5	10800	124160	5.9	10800	124160	4.9	10801
7	2/2/10/2	117630	0.6	10800	117630	0.6	10800	117630	0.6	10801
8	2/2/10/4	138460	1.8	10800	138360	2.3	10800	138360	1.3	10801
9	2/2/10/6	156702	5.0	10800	156750	5.5	10800	161850	10.6	10801
10	2/4/2/2	84250	0.0	336	84250	0.0	862	84250	0.0	472
11	2/4/2/4	97500	1.3	10800	97500	1.4	10800	97500	0.0	2951
12	2/4/2/6	110750	3.0	10800	110750	3.1	10800	110750	3.5	10801
13	2/4/6/2	105715	1.0	10800	105715	1.1	10800	105715	1.0	10801
14	2/4/6/4	129255	6.6	10800	127340	5.4	10800	127340	4.7	10801
15	2/4/6/6	163250	24.0	10800	160975	22.9	10810	148255	8.8	10800
16	2/4/10/2	123830	4.5	10800	122370	3.8	10800	122370	1.1	10801
17	2/4/10/4	167485	17.0	10800	152015	9.0	10800	148590	6.4	10801
18	1/1/3/2	66070	0.0	1	66070	0.0	2	66070	0.0	2
19	1/1/3/2	67080	0.0	1	67080	0.0	3	67080	0.0	18
20	1/1/4/2	78080	0.0	5	78080	0.0	7	78080	0.0	5
21	1/2/2/1	67260	0.0	2	67260	0.0	7	67260	0.0	7
22	1/2/2/2	82970	0.0	62	82970	0.0	67	82970	0.1	10801
23	1/2/2/3	75140	0.0	8	75140	0	74	75140	0.0	36
24	2/2/2/2	81900	0.9	10800	81900	0.9	10800	81900	0.3	10801
25	2/2/4/2	87840	1.5	*3832	87840	1.5	*3815	87840	1.4	10801
26	2/2/6/2	86170	0.4	10800	86170	0.4	10800	86170	0.3	10801

at an intersection of two TEN-T corridors.

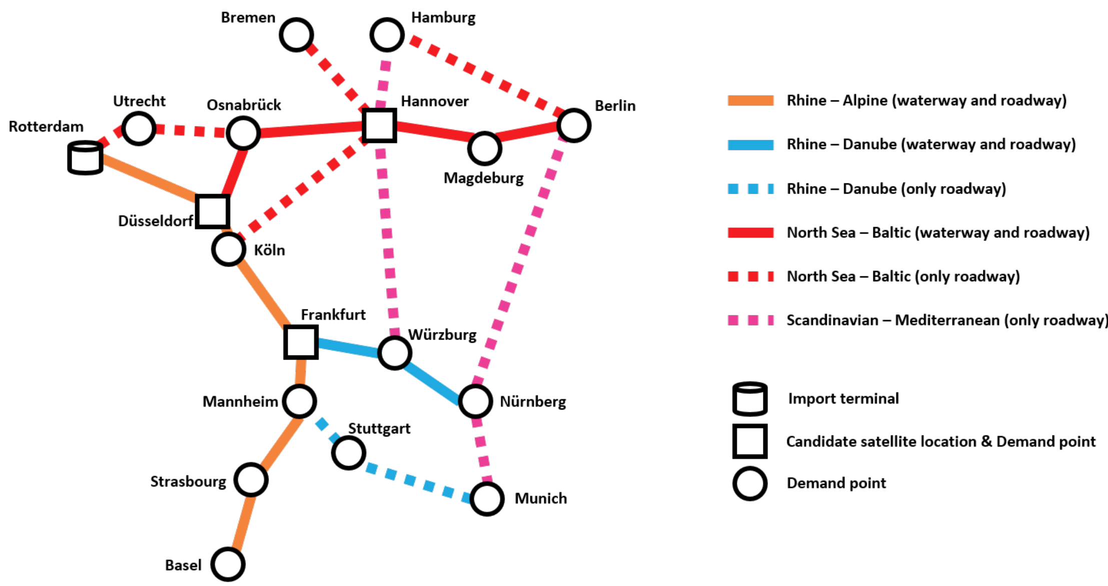

Figure 5: The part of the TEN-T core network considered in the case study

We rely on several sources of data and observations in practice for creating scenarios that reflect the current and planned development of the supply chain for LNG as a fuel in Europe. The Netherlands has been a front runner in developing the supply chain for LNG as a fuel, with 25 LNG fuel stations and 7 port locations being operational by the end of 2018. These numbers are increasing, and the network of fuel stations locations for bunkering is expanding into Europe. To reflect this growth, our case study considers three different supply chain maturity phases, during which the network grows from 8 to 14, to 18 demand points, and three different demand scenarios (i.e., low, medium, high) as shown in Figure 6. Throughout the experiments, we consider a time horizon of 10 weeks, consisting of 5 periods of two weeks. These two-week periods are chosen to reflect the typical replenishment cycle of LNG fuel stations and bunkering of ships that sail on LNG as a fuel.

Given the very large investments involved with opening an LNG import terminal, and due to its much broader purpose than providing LNG as a fuel, only a fraction of the investment and operational costs translate into costs relevant for the supply chain for LNG as a fuel. Our experimental design follows the current state of practice, where specific terminal investments related to facilitating LNG as a fuel are translated into a fixed fee for bunker barges and tanker trucks when they load the fuel at the terminal. These so-called slot costs are roughly €20,000 for a bunker barge, and €500 for tanker trucks. In 2018, two bunker barges were under construction for the European LNG supply chain. None were yet in use. For the purpose of our case study, we consider a capacity of $2000m^3$, which resembles the capacity of the "Clean Jacksonville", the first LNG bunker barge built in North America, which was delivered by the end of 2018. The capacity of a tanker truck is $50m^3$. Note that the slot cost per m^3 of LNG are equal for the tanker truck and bunker barge when they are fully loaded.

The initial investment associated with opening a satellite with a capacity of $300m^3$ is estimated at €1,000,000. The satellite capacity can be upgraded with at most two modules of $300m^3$ at a cost of €500,000 each. Developing the site for a satellite (e.g., acquiring permits,

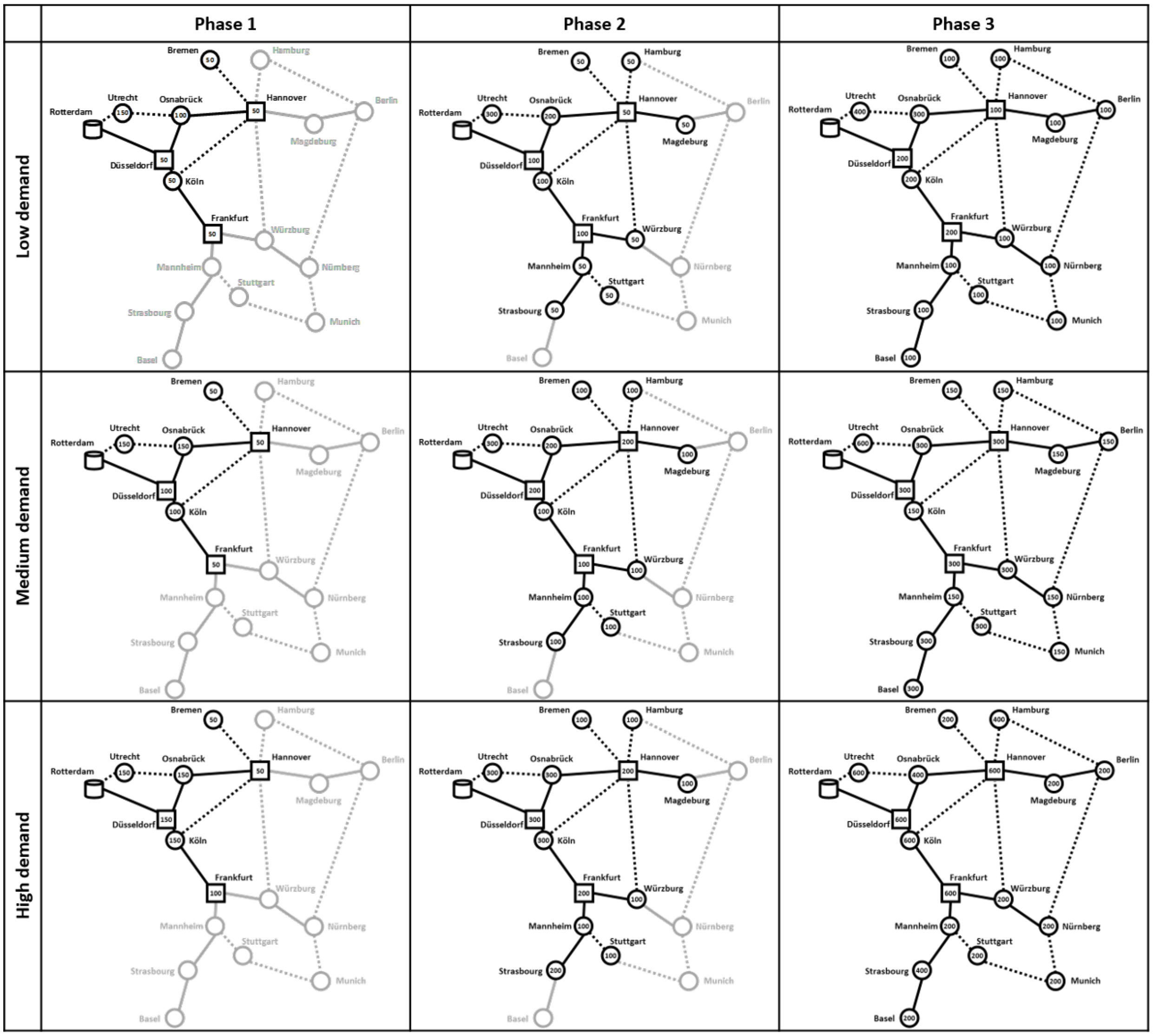

Figure 6: Demand scenarios

foundations, piping) makes up a considerable part of the total investment, which is why upgrading a satellite is far less expensive than opening one. Tanker trucks for transporting cryogenic liquids (such as LNG) are widely available. We consider a cost of €1.5 per kilometer for using a tanker truck, which is based on a full operational lease price for such a vehicle, including initial investment, maintenance and all operational costs. Since the capacity of tanker trucks often does not allow for replenishing multiple LNG demand points, we consider only direct vehicle routes from a facility to a demand point in the case study. The initial investment of an LNG bunker barge is estimated at €5,000,000; its variable costs per kilometer at €7. We translated the investment costs of satellites and bunker barges into periodic costs by computing constant payments over a depreciation period of 30 years, an interest rate of 5% and a scrap value of 20% of the initial investment. This results in a period investment cost of €11,930 for a bunker barge, and €2,386 for a satellite.

The problem considered in this case study is a special case of the problem described in Section 2, as we investigate an LNG network where decisions regarding the establishment of import terminals are predefined. Furthermore, we note that split deliveries play a critical role in the case study since a single tanker truck is seldom large enough to fulfill the demand of a customer in a period. This implies that demand points served from a satellite facility would require split deliveries in most cases.

5.1. Results

An overview of the results for the nine cases, each with a different supply chain maturity phase and demand scenario, can be found in Table 6. In this table, we show which satellites open in each scenario (between parenthesis, we show the number of upgrade modules for each open satellite).

Table 6: An overview of the case study results

Instance	Hannover	Frankfurt	Dusseldorf	Barges	Cost per m^3
Low 1	Closed (0)	Closed (0)	Closed (0)	0	€29.4
Low 2	Closed (0)	Closed (0)	Closed (0)	0	€30.4
Low 3	Open (1)	Open (2)	Closed (0)	1	€30.8
Medium 1	Closed (0)	Closed (0)	Closed (0)	0	€28.6
Medium 2	Open (2)	Open (2)	Closed (0)	1	€34.2
Medium 3	Open (2)	Open (2)	Closed (0)	2	€30.0
High 1	Closed (0)	Closed (0)	Closed (0)	0	€29.1
High 2	Open (1)	Open (1)	Closed (0)	1	€28.5
High 3	Open (2)	Open (2)	Closed (0)	2	€30.1

Using the cost and capacity values mentioned above, no satellites are opened in the least mature supply chain phase (i.e., Phase 1) in any of the demand scenarios. In the most mature supply chain phase (i.e., Phase 3), two satellites are opened: one in Hannover, and one in Frankfurt. Both satellites receive one capacity upgrade in the low demand scenario, and two in the medium and high demand scenarios. In maturity Phase 2, no satellites are opened in the low demand scenario, while Hannover and Frankfurt are opened for the medium and high demand scenarios.

Each case where a satellite is opened also involves the use of one or two bunker barges, which is logical since satellites can only be replenished by a bunker barge. While bunker barges could also be used without an open satellite in the network, the case study results show that bunker barges are only used when at least one satellite is opened. Our analysis indicates that a bunker barge generally uses most of its capacity to replenish the satellite(s), and visits a few demand points with the remainder of its load. Due to the relatively high slot costs, the barge is filled to maximum capacity at the import terminal.

What is noticeable in Table 6, is that the total cost per m^3 of demand is relatively stable. This implies that the cost increase that is to be expected when LNG needs to be transported further from the import terminal can be largely mitigated by investing in one or more bunker barges and satellites.

5.2. Sensitivity analysis

We conducted a sensitivity analyses to gain further insights into the role of different cost components and capacities of the satellites and fleets of vehicles. We were particularly interested to study the impact of the investment costs associated with satellites and bunker barges since these costs are seldom formally documented and yet may have a large impact on the network design decisions. Specifically, we consider the situation when the investment in a bunker barge would be €3,000,000 or €10,000,000 ceteris paribus. Similarly, we consider the situation when the investment involved in opening a satellite would be €500,000 or €2,000,000, while the upgrade costs remain half the initial investment per module. We also study the effect of the costs for using tanker trucks (i.e., either €0.75 or €3 per kilometer). Lastly, to study the impact of the capacity of the bunker barge, we consider the situation where the capacity would be $1000m^3$ or $3000m^3$, while adjusting the slot costs and investment costs so that they remain equal per m^3 of capacity.

The results from the sensitivity analyses show that the network designs are robust to changes in the investment costs for the bunker barge. Our algorithm identifies exactly the same network designs as best solution for all nine cases when considering lower bunker barge investment costs. At higher bunker barge investment costs, the use of bunker barges and satellites is somewhat postponed, indicated by the fact that no satellites or bunker barges are used in the medium demand scenarios for maturity phases 1 and 2. The results behave similarly to changes in the investment costs associated with opening and upgrading satellites. Of course, the total supply chain costs are higher or lower due to the differences in investment costs associated with bunker barges or satellites, but overall, the routing costs appear to be a larger part of the total supply chain costs.

It is therefore not surprising that the case study results are more sensitive to the variable costs associated with using the vehicles, and the capacity of the bunker barges. When the use of tanker trucks is cheap (i.e., when the variable costs amount to €0,75 per kilometer), our algorithm identifies the solution without any satellites and bunker barges as the best network design. High variable costs for the tanker trucks (i.e., €3 per kilometer) result in network designs with (larger) satellites opening in lower demand scenarios and earlier supply chain maturity phases.

The capacity of the bunker barges also affects the network designs. Smaller capacity of the bunker barges leads to either an extra bunker barge being operational, and hence, an increase in the variable routing costs associated with barge usage; or a lower number of satellites, while a larger part of the network is serviced by tanker trucks from the import terminal. When the capacity of bunker barges is large, it becomes more cost-effective to service larger parts of the network by means of one barge. Satellites are then opened only in the higher demand scenarios and more mature supply chain phases, to service mostly those nodes that are not connected by means of waterways. Overall, the cost savings that can be made by improving the routes of the different vehicles in the network quickly outweigh the additional investments needed to open and upgrade satellites and use bunker barges.

6. Conclusions

Inspired by a real-world network design problem related to the expansion of the European supply chain for LNG as a fuel, this paper introduces the Two-Echelon Location Routing Problem with Split Deliveries. Allowing direct shipments from terminals at different levels of the LNG supply chain to the costumers makes this location routing problem complex to solve. We have improved the performance of a hybrid exact algorithm, which outperforms its previous version and a commercial solver. A detailed case study sheds light on the development of opening satellite terminal(s) and investing in bunker barges when expanding the supply chain for LNG as a fuel into Europe.

References

[1] Akca, Z., Berger, R., Ralphs, T., 2008. Modeling and solving location routing and scheduling problems. In: Proceedings of the eleventh INFORMS computing society meeting. pp. 309–330.

[2] Albareda-Sambola, M., Diaz, J. A., Fernández, E., 2005. A compact model and tight bounds for a combined location-routing problem. Computers & Operations Research 32 (3), 407–428.

[3] Albareda-Sambola, M., Fernández, E., Nickel, S., 2012. Multiperiod location-routing with decoupled time scales. European Journal of Operational Research 217 (2), 248–258.

[4] Balakrishnan, A., Ward, J., Wong, R., 1987. Integrated facility location and vehicle routing models: Recent work and future prospects. American Journal of Mathematical and Management Sciences 7 (1-2), 35–61.

[5] Baldacci, R., Mingozzi, A., Wolfler Calvo, R., 2011. An exact method for the capacitated location-routing problem. Operations Research 59 (5), 1284–1296.

[6] Barreto, S. d. S., 2004. Análise e modelização de problemas de localização-distribuição. tese de doutoramento, Gestao Indústrial, Universidade de Aveiro, Aveiro, Portugal.

[7] Boventer, E., 1961. The relationship between transportation costs and location rent in transportation problems. Journal of Regional Science 3 (2), 27–40.

[8] Contardo, C., Cordeau, J.-F., Gendron, B., 2013. An exact algorithm based on cut-and-column generation for the capacitated location-routing problem. INFORMS Journal on Computing 26 (1), 88–102.

[9] Cuda, R., Guastaroba, G., Speranza, M. G., 2015. A survey on two-echelon routing problems. Computers & Operations Research 55, 185–199.

[10] Drexl, M., Schneider, M., 2015. A survey of variants and extensions of the location-routing problem. European Journal of Operational Research 241 (2), 283–308.

[11] Duarte, A., Mladenović, N., Sánchez-Oro, J., Todosijević, R., 2016. Variable neighborhood descent. In: Martí, R., Panos, P., Resende, M. G. (Eds.), Handbook of Heuristics. Springer International Publishing, Cham, pp. 1–27.

[12] Escobar, J. W., Linfati, R., Baldoquin, M., Toth, P., 2014. A granular variable tabu neighborhood search for the capacitated location-routing problem. Transportation Research Part B: Methodological 67, 344–356.

[13] Guastaroba, G., Speranza, M. G., Vigo, D., 2016. Intermediate facilities in freight transportation planning: a survey. Transportation Science 50 (3), 763–789.

[14] Hof, J., Schneider, M., Goeke, D., 2017. Solving the battery swap station location-routing problem with capacitated electric vehicles using an avns algorithm for vehicle-routing problems with intermediate stops. Transportation Research Part B: Methodological 97, 102–112.

[15] Karaoglan, I., Altiparmak, F., Kara, I., Dengiz, B., 2012. The location-routing problem with simultaneous pickup and delivery: Formulations and a heuristic approach. Omega 40 (4), 465–477.

[16] Koç, Ç., Bektaş, T., Jabali, O., Laporte, G., 2016. The impact of depot location, fleet composition and routing on emissions in city logistics. Transportation Research Part B: Methodological 84, 81–102.

[17] Lahyani, R., Coelho, L. C., Renaud, J., 2018. Alternative formulations and improved bounds for the multi-depot fleet size and mix vehicle routing problem. OR Spectrum 40 (1), 125–157.

[18] Laporte, G., Nobert, Y., Taillefer, S., 1988. Solving a family of multi-depot vehicle routing and location-routing problems. Transportation Science 22 (3), 161–172.

[19] Larrain, H., Coelho, L. C., Cataldo, A., 2017. A variable mip neighborhood descent algorithm for managing inventory and distribution of cash in automated teller machines. Computers & Operations Research 85, 22–31.

[20] Maranzana, F. E., 1964. On the location of supply points to minimize transport costs. Journal of the Operational Research Society 15 (3), 261–270.

[21] Menezes, M., Ruiz-Hernández, D., Verter, V., 2016. A rough-cut approach for evaluating location-routing decisions via approximation algorithms. Transportation Research Part B: Methodological 87, 89–106.

[22] Min, H., Jayaraman, V., Srivastava, R., 1998. Combined location-routing problems: A synthesis and future research directions. European Journal of Operational Research 108 (1), 1–15.

[23] Mladenović, N., Hansen, P., 1997. Variable neighborhood search. Computers & Operations Research 24 (11), 1097–1100.

[24] Nagy, G., Salhi, S., 2007. Location-routing: Issues, models and methods. European Journal of Operational Research 177 (2), 649–672.

[25] Perl, J., Daskin, M. S., 1985. A warehouse location-routing problem. Transportation Research Part B: Methodological 19 (5), 381–396.

[26] Post, R. M., Buijs, P., uit het Broek, M. A., Alvarez, J. A. L., Szirbik, N. B., Vis, I. F., 2018. A solution approach for deriving alternative fuel station infrastructure requirements. Flexible Services and Manufacturing Journal 30 (3), 592–607.

[27] Prins, C., Prodhon, C., Ruiz, A., Soriano, P., Wolfler, Calvo, R., 2007. Solving the capacitated location-routing problem by a cooperative lagrangean relaxation-granular tabu search heuristic. Transportation Science 41 (4), 470–483.

[28] Prins, C., Prodhon, C., Wolfler, Calvo, R., 2006. Solving the capacitated location-routing problem by a grasp complemented by a learning process and a path relinking. 4OR 4 (3), 221–238.

[29] Prodhon, C., 2011. A hybrid evolutionary algorithm for the periodic location-routing problem. European Journal of Operational Research 210 (2), 204–212.

[30] Prodhon, C., Prins, C., 2014. A survey of recent research on location-routing problems. European Journal of Operational Research 238 (1), 1–17.

[31] Rieck, J., Ehrenberg, C., Zimmermann, J., 2014. Many-to-many location-routing with inter-hub transport and multi-commodity pickup-and-delivery. European Journal of Operational Research 236 (3), 863–878.

[32] Santos, F., Mateus, G., da Cunha, A., 2015. A branch-and-cut-and-price algorithm for the two-echelon capacitated vehicle routing problem. Transportation Science 49 (2), 355–368.

[33] Schiffer, M., Walther, G., 2018. Strategic planning of electric logistics fleet networks: A robust location-routing approach. Omega 80, 31–42.

[34] Schneider, M., Löffler, M., 2017. Large composite neighborhoods for the capacitated location-routing problem. Transportation Science 53 (1), 301–318.

[35] Thunnissen, S., van de Bunt, L., Vis, I., 2016. Sustainable fuels for the transport and maritime sector: A blueprint of the LNG distribution network. In: Logistics and Supply Chain Innovation. Springer, pp. 85–103.

[36] Tuzun, D., Burke, L. I., 1999. A two-phase tabu search approach to the location routing problem. European Journal of Operational Research 116 (1), 87–99.

[37] Watson-Gandy, C. D. T., Dohrn, P. J., 1973. Depot location with van salesmen – a practical approach. Omega 1 (3), 321–329.